Advances in Nano Research, *Vol. 18, No. 5 (2025) 445-458*
https://doi.org/10.12989/anr.2025.18.5.445

Stability analysis of nano-devices: Exercise-mediated effects on nanodevice stability in drug delivery applications

Huanan Chen*[1], Jiahao Zhu[2], Mostafa Habibi[3,4,5], Ameni Brahmia[6] and Dan Wnag[7]

[1]*College of Ministry of sports, Namseoul University, Cheonan City, South Chungcheong, 31020, Korea*
[2]*College of Ministry of sports, Dankook University, Yongin-si, Gyeonggi-do, 16890, Korea*
[3]*Universidad UTE, Facultad de Arquitectura y Urbanismo, Calle Rumipamba S/N y Bourgeois, Quito 170147, Ecuador*
[4]*Department of Biomaterials, Saveetha Dental College and Hospital, Saveetha Institute of Medical and Technical Sciences, Chennai 600 077, India*
[5]*Institute of Research and Development, Duy Tan University, Da Nang 550000, Viet Nam*
[6]*Department of Chemistry, College of Science, King Khalid University, P.O. Box 9004, 61413 Abha, Saudi Arabia*
[7]*Institute Sciences and Design of AL-Kharj, Dubai, United Arab Emirates*

(*Received May 24, 2023, Revised March 18, 2025, Accepted March 19, 2025*)

Abstract. This study examines the relationship between physical exercise and the stability of nanodevices intended for targeted drug-delivery systems, emphasizing applications in sports science and medicine. The hemodynamic changes resulting from physical activity, including fluctuations in blood flow velocity and pressure, are essential factors affecting the performance and stability of nanodevices in the bloodstream. A modified continuum modeling approach that integrates high-order beam theory and nonlocal strain gradient theory is employed to simulate the dynamic behavior of nanodevices with nonuniform tubular geometries. The proposed design of the nanodevice includes a central nanomotor and two truncated conical nanotubes, functioning as nanoblades for the accurate transport and release of therapeutic agents. Numerical simulations investigate the nanodevice's rotational and vibrational stability under physiologically relevant conditions, such as changes in physical training intensity and blood flow patterns. This study thoroughly explores how essential aspects such as device design, material properties, and exercise-induced hemodynamic forces affect nanodevice performance. The results are corroborated by existing published data, indicating the potential for improved drug-delivery efficiency in active individuals. This research integrates mechanical engineering principles with sports science to establish a framework for developing advanced nanodevices suited to dynamic physiological environments, which has important implications for sports medicine, rehabilitation, and personalized healthcare.

Keywords: blood flow dynamics; continuum modeling; drug delivery; exercise hemodynamics; nanodevice stability; physical training

1. Introduction

The incorporation of nanoscience into bioengineering has revolutionized the creation of advanced materials and devices for biomedical use. Researchers have extensively investigated nanotechnology's ability to manipulate matter at the atomic and molecular levels, allowing for the development of novel systems to address critical challenges in healthcare, sports science, and rehabilitation (Ye *et al*. 2023, Zhao *et al*. 2023, Shen *et al*. 2024). Li *et al*. (2022) utilized a two-dimensional continuum mechanics framework to model the bending responses of higher-order annular plates, with the objective of evaluating the mechanical durability and functional adaptability of graphene-reinforced nanomaterials. Dai *et al*. (2021) performed sensitivity analyses on size-dependent laminated nanoshells to highlight their applicability in bioengineering. In recent years, nanoscience has been used in bioengineering to develop wearable sensors, drug delivery systems, and sports equipment. Wang *et al*. (2025a) studied nanoparticle-infused oils for better lubrication in automotive parts, demonstrating nanomaterials' versatility in a variety of applications. The advancements in nanoscience highlight its pivotal role in creating multifunctional systems capable of addressing intricate biological and physiological requirements. Nanotechnology has emerged as a leading force in bioengineering innovations owing to its ability to create nanoscale components with tailored attributes, such as enhanced biocompatibility, flexibility, and strength (Mirjavadi *et al*. 2020b, c, d, e). The literature reveals a growing emphasis on combining nanotechnology and bioengineering principles to solve real-world problems. Huo *et al*. (2021) studied the bending behavior of functionally graded graphene platelet-reinforced composite (FG-GPLRC) plates using 3D-poroelasticity theory, emphasizing their potential in load-bearing applications. Similarly, Zhang *et al*. (2021) investigated low-velocity impact responses of viscoelastic panels, demonstrating nanocomposite structures' resilience in dynamic conditions. These studies demonstrate the importance of nanomaterials in improving structural integrity and performance (Mirjavadi *et al*. 2020a, 2022a, b, c, Afshari Behzad *et al*.

*Corresponding author, Ph.D.,
E-mail: 15896817387@163.com

ISSN: 2287-237X (Print), 2287-2388 (Online)

2022, Kazemi *et al*. 2023, 2024, Mirjavadi *et al*. 2023). Furthermore, Habibi and colleagues have made significant contributions to this field through their research into smart materials and adaptive systems. Zhu *et al*. (2024b) investigated bulk wave dispersion in poroelastic beams during athletic training, demonstrating the optimization of nanomaterials for biomechanical applications. Wang *et al*. (2024d) made a substantial contribution by investigating the energy absorption characteristics of vibrating sports equipment, thereby validating the effectiveness of nano-engineered materials in high-performance applications (Zhao *et al*. 2024). Despite these advancements, there are still challenges in scaling up nanotechnological solutions while maintaining cost-effectiveness and safety (Lei *et al*. 2022, Wu *et al*. 2023, 2024). According to Man *et al*. (2024), synthesizing magnetic nanocatalysts for biodiesel production necessitated meticulous parameter optimization, including temperature and pressure. This underscores the need for continued research into scalable manufacturing techniques that preserve the unique properties of nano-materials (Zhu *et al*. 2022). Furthermore, Song *et al*. (2024) used the Hashin-Shtrikman bounds homogenization model to investigate the frequency responses of imperfect functionally graded bio-composite plates, emphasizing the significance of combining advanced numerical methods with experimental data (Zhang *et al*. 2024c).

The advancement of nano-devices for drug delivery represents a noteworthy progression in the field of bio-medicine, as investigators examined innovative methodologies to enhance patient outcomes and therapeutic effectiveness (Liang *et al*. 2024, Wang *et al*. 2024a, b, 2025b, Yan *et al*. 2024). These devices seek to overcome the shortcomings inherent in conventional drug delivery systems, such as systemic toxicity, inadequate targeting, and diminished bio-availability (Zhang *et al*. 2021). Nano-devices demonstrate the capability to traverse complex biological barriers, including the blood-brain barrier and dense tumor tissues, due to their diminutive size and elevated surface-area-to-volume ratio (Dai *et al*. 2021). This capability enabled precise regulation of therapeutic agent release, ensuring that medications effectively reached their intended targets while minimizing side effects (Shi *et al*. 2022). Recent advancements in nanostructured architectures have expanded the use of nano-devices in drug delivery systems. For instance, nanoparticles have been engineered to encapsulate both hydrophobic and hydrophilic drugs, allowing researchers to refine release kinetics and achieve extended therapeutic effects (Wang *et al*. 2022, Jia *et al*. 2023, Zhang *et al*. 2023a, b, c, Liang *et al*. 2024, Qi *et al*. 2024). This precise and targeted drug delivery system effectively reduced drug-related toxicity while also improving patient adherence through a decrease in dosing frequency (Chen *et al*. 2022). Nano-devices demonstrated significant potential in cancer therapy by acting as platforms for the targeted delivery of tumor-specific drugs, thereby improving treatment efficacy and reducing side effects. The literature presented significant evidence of the adaptability and effectiveness of nano-devices in drug delivery applications. Wang *et al*. (2024a) conducted a study modeling the bending responses of graphene-reinforced higher-order annular plates, emphasizing their applicability in load-bearing roles within drug delivery systems. Li *et al*. (2024b) performed sensitivity tests on size-dependent laminated nanoshells, demonstrating their efficacy in encapsulating and delivering therapeutics. Xue *et al*. (2024) made an important contribution by studying the low-velocity impact and resonance properties of viscoelastic panels augmented with graphene nanoplatelets. Their findings suggested that these materials could be modified for use in dynamic physiological environments like the bloodstream, where stability and reactivity are critical. Zhu *et al*. (2024b) investigated the energy absorption properties of vibrating sports equipment, demonstrating the versatility of nano-engineered materials in a variety of applications, including drug delivery. Despite these advances, there are still challenges in optimizing nanodevices for specific applications. Ma *et al*. (2024) demonstrated that synthesizing magnetic nanocatalysts for biodiesel production necessitated meticulous parameter optimization, such as temperature and pressure. Similarly, designing nano-devices for drug delivery necessitated careful consideration of factors such as biocompatibility, degradation rates, and interactions with living systems (Li *et al*. 2024a). Addressing these issues was essential for transforming laboratory innovations into clinically viable solutions. Recent studies emphasize the significance of mathematical formulations in enhancing the accuracy of stability analyses (Wang *et al*. 2023, 2024h, Xia *et al*. 2024). Wang *et al*. (2024c) employed the Hashin-Shtrikman bounds homogenization model to analyze the frequency responses of defective functionally graded bio-composite plates, highlighting the significance of integrating advanced numerical methods with empirical data (Wang *et al*. 2024f). These methodologies allowed for more accurate predictions of nano-device effectiveness in practical applications (Zhu *et al*. 2024a). Additionally, researchers investigated the use of artificial intelligence (AI) to predict the behavior of nano-devices. Zhang *et al*. (2024b) created AI-driven models to predict linear and nonlinear buckling in nonuniform functionally graded micro-tubes, which were then adapted for use in sports training equipment. Likewise, Zhao *et al*. (2024) employed neural-fuzzy systems to evaluate the formability of St14 steel sheets, illustrating the capacity of AI in enhancing nano-device design. These innovations highlighted the pivotal role of interdisciplinary methods in enhancing drug delivery technologies. Huang *et al*. (2024) examined electroelastic wave dispersion in rotary piezoelectric NEMS sensors, providing insights for the optimization of nano-devices in real-time drug delivery monitoring. Man *et al*. (2024) developed a stretchable-thickness model to examine the dynamic responses of graphene origami-reinforced sport plates, thereby enhancing the application of mechanical engineering principles in the investigation of nano-devices (Wang *et al*. 2024e). The studies collectively emphasized the significance of integrating advanced materials and computational tools to improve the functionality of nano-devices (Wang *et al*. 2024g, 2025c, Zhao *et al*. 2025). Despite these advancements, researchers encountered persistent difficulties in scaling nano-devices for extensive clinical application. Zhiqiang *et al*. (2024) highlighted that the analysis of bulk wave

propagation in imperfect FG bio-composite beams indicates a necessity for enhanced manufacturing techniques to achieve consistent performance (Zisong and Habibi 2024). Guo *et al*. (2024) highlighted the significance of enhancing dynamic stability in spinning FG-piezoelectric cylindrical structures, indicating that additional refinements are required for optimal outcomes (Wang *et al*. 2024b). Jin *et al*. (2024) performed semi-analytical stability analyses of composite concrete structures, providing important insights into the structural integrity of nano-devices under different conditions. Yu *et al*. (2024) investigated DNS key technologies utilizing machine learning, highlighting the efficacy of data-driven methods in enhancing nano-device performance (Xiao *et al*. 2024). These contributions collectively enhanced the field, facilitating the development of more robust and reliable drug delivery systems.

The effect of exercise and physical training on drug delivery systems has garnered more attention in recent years, with researchers striving to understand how physiological changes during physical activity influence medication pharmacokinetics and pharmacodynamics (Hao *et al*. 2024, Yang *et al*. 2025, Zhou *et al*. 2025). Physical activity affects hemodynamics, causing increased blood flow velocity and pressure gradients that may have a significant influence on pharmaceutical distribution, absorption, and metabolism in the body. The modifications are particularly relevant for nano-devices designed for targeted drug delivery, as they operate in dynamic physiological environments where exercise-induced pressures may influence their stability and efficacy. Limited research indicates that exercise may improve the absorption of drugs delivered through transdermal patches, potentially leading to drug toxicity and serious outcomes. Exercise-induced decreases in hepatic blood flow alter how medications with high clearance rates, such as lidocaine and nitrates, are metabolized. This underscores the need of considering exercise-induced effects when developing medicine delivery systems (Wang *et al*. 2024a). Furthermore, research has shown that physical activity might enhance mental health by lowering anxiety and depression, which may have an indirect impact on medication efficacy and adherence. The literature provides substantial evidence regarding the interaction between physical exercise and pharmacokinetic processes. Studies demonstrate that exercise programs markedly decrease drug cravings in individuals undergoing addiction treatment, highlighting the potential of physical activity as a supplementary therapy. Studies have shown that exercise can affect the pharmacokinetics of certain medications by altering blood flow dynamics and tissue perfusion. Exercise has a significant influence on hemodynamics, especially in nano-devices. Zhu *et al*. (2024b) explored bulk wave dispersion in poroelastic beams relevant to athletic training, showing the potential for improving nanomaterials in biomechanical applications. Their results demonstrated that understanding the correlation between exercise-induced stresses and the stability of nano-devices is crucial for guaranteeing dependable medication delivery. Notwithstanding these breakthroughs, obstacles remain in forecasting and alleviating the impacts of activity on medicine delivery systems. Man *et al*. (2024) demonstrate that the synthesis of magnetic nanocatalysts for biodiesel production requires careful optimization of parameters, including temperature and pressure. The design of nano-devices for drug administration requires careful consideration of biocompatibility, degradation rates, and interactions with biological systems (Omidi *et al*. 2013, Mousavi *et al*. 2017, Shahabinejad *et al*. 2018). Addressing these issues was essential for translating laboratory advancements into clinically applicable treatments. Recent research underscores the importance of mathematical formulations in enhancing the accuracy of stability analyses. Song *et al*. (2024) employed the Hashin–Shtrikman bounds homogenization model to analyze the frequency responses of flawed functionally graded bio-composite plates, highlighting the importance of integrating advanced numerical methods with empirical data. These techniques facilitated more dependable forecasts of nano-device stability in real applications (Ma *et al*. 2024). Furthermore, researchers investigated the incorporation of artificial intelligence (AI) in forecasting the behavior of nano-devices. Zhang *et al*. (2024b) created AI-driven models to forecast linear and nonlinear buckling in nonuniform functionally graded micro-tubes, later modifying these models for use in sports training apparatus. Zisong and Habibi (2024) used neural-fuzzy systems to evaluate the formability of St14 steel sheets, illustrating the capability of artificial intelligence in enhancing nano-device design. The advancements highlighted the need of interdisciplinary methods in enhancing pharmaceutical delivery technology. The propagation of electroelastic waves in rotary piezoelectric NEMS sensors was the subject of an investigation by Guo *et al*. (2024). The research offered significant insights for the advancement of nano-devices in real-time medication delivery monitoring. Wang *et al*. (2024b) analyzed the dynamic responses of graphene origami-reinforced sport plates using a stretchable-thickness model, demonstrating the significance of mechanical engineering principles in nano-device research. This study highlights the importance of employing modern computational methods and materials to improve the performance of nano-devices. Despite these promising discoveries, researchers faced ongoing challenges in scaling nano-devices for wider therapeutic applications. Xiao *et al*. (2024) highlighted the necessity for enhanced manufacturing techniques to achieve consistent performance in the study of bulk wave propagation in defective FG bio-composite beams. Zhang *et al*. (2024a) emphasized the necessity of improving dynamic stability in rotating FG-piezoelectric cylindrical structures, suggesting that further enhancements were required for optimal results. He *et al*. (2024) conducted semi-analytical stability evaluations of composite concrete structures, yielding important insights into the structural integrity of nano-devices across various conditions. Liu *et al*. (2024) examined critical technologies in DNS through machine learning, emphasizing the effectiveness of data-driven approaches in improving the performance of nano-devices. Their contributions collectively advanced the field, enabling the creation of more robust and reliable drug delivery systems.

Notwithstanding the considerable progress achieved in

the utilization of nanotechnology for drug delivery systems, numerous deficiencies and voids persist within the current body of literature. Previous research has largely concentrated on static environments, overlooking the dynamic physiological conditions brought about by physical exercise and hemodynamic fluctuations. This oversight undermines the reliability of nano-devices in practical applications, where variables like blood flow velocity, pressure gradients, and mechanical vibrations can considerably affect their stability and performance. Furthermore, although previous studies have investigated the mechanical properties of nanomaterials, there is a lack of research that combines advanced continuum mechanics, nonlocal strain gradient theory, and numerical simulations to thoroughly assess the stability of nano-devices subjected to exercise-induced forces. This study addresses existing deficiencies by applying an enhanced continuum modeling technique that integrates high-order beam theory with nonlocal strain gradient theory to simulate the dynamic characteristics of nonuniform tubular nano-devices effectively. This study examines the effects of exercise-induced hemodynamic changes on the rotational and vibrational stability of nanoscale devices designed for targeted drug delivery. Moreover, the suggested design, incorporating a central nanomotor and truncated conical nanotubes acting as nanoblades, presents an innovative framework for the meticulous transport and regulated release of therapeutic agents. Through the validation of findings against established published data, this research not only confronts significant limitations present in earlier studies but also lays the groundwork for the advancement of sophisticated nano-devices designed for dynamic physiological contexts, carrying profound implications for sports medicine, rehabilitation, and personalized healthcare. This ground-breaking fusion of mechanical engineering concepts with sports science highlights the originality of the present research, establishing it as a significant advancement in the domain of nanotechnology-enabled drug delivery systems.

2. Presentation of mathematical modeling of nano-devices for drug delivery based on mechanical engineering

The stability of nanoparticles in drug delivery applications directly influences the accuracy and reliability of therapeutic substance delivery and discharge. Nano-devices, such as core nanomotors and truncated conical nanotubes, exhibit considerable potential for improving targeted drug delivery by effectively navigating complex physiological environments and overcoming biological barriers. Nonetheless, the dynamic restrictions imposed by these conditions, especially exercise-induced hemodynamic changes, may influence the efficacy and stability of nanodevices. Variations in blood flow velocity, pressure gradients, and mechanical vibrations caused by physical activity may affect the rotational and vibrational stability of nanodevices designed for precise control. Comprehending the effects of exercise-induced stresses on nanodevice design and material properties is crucial for ensuring

Fig. 1 Schematic representation of nano-devices in drug delivery applications

reliable performance in practical applications. This section combines the theoretical principles of nano-device stability with practical applications, using advanced mechanical engineering models to predict and assess the impact of physical training on drug delivery systems. Thus, it will be feasible to develop designs specifically adapted to varying physiological conditions. Nano-devices signify substantial progress in drug delivery systems, enabling exact control over the transport and release of therapeutic substances. Fig. 1 illustrates that these devices use their small size, high surface-area-to-volume ratio, and enhanced material properties to navigate complex biological obstacles and achieve precise delivery. The illustration provides a conceptual framework for the operation of nano-devices in the human body, emphasizing their potential to enhance medication bioavailability, minimize off-target effects, and adapt to fluctuating physiological circumstances.

The mathematical modeling of nanodevices for drug delivery applications signifies a crucial convergence of mechanical engineering concepts with biomedical innovation. Utilizing sophisticated continuum mechanics, nonlocal strain gradient theory, and higher-order beam theories, researchers can model the dynamic behavior of nano-devices under diverse physiological situations. These models include size-dependent effects, material characteristics, and external forces, enabling accurate predictions of stability, rotational dynamics, and vibrational responses. The use of nonlocal strain gradient theory facilitates precise modeling of nanoscale phenomena, including the effects of surface energy and interatomic interactions, sometimes overlooked in classical mechanics. Moreover, these mathematical frameworks provide a basis for enhancing nano-device design, guaranteeing their efficacy in intricate settings such as the bloodstream, where hemodynamic forces and exercise-induced variations are pivotal.

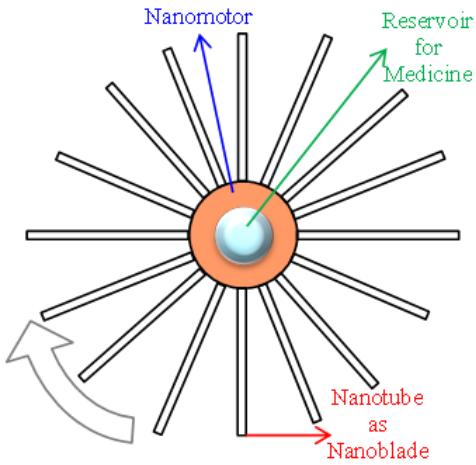

Fig. 2 Schematic representation of rotating nanotube via nanomotor

2.1 Description of the system

A nanotube is considered as a nanomotor blade, with one end fixed to a nanomotor and the other free to rotate around an axis. The nanotube has a length 'L', an internal radius 'R_i', and an external radius 'R_e'. A tank or reservoir within the nanomotor is designed to carry nanomedicine (Fig. 2). The nanomotor spins around an axis, using the nanotube as its blade. The mathematical model for the blade's motion is based on principles of mechanical engineering. To derive the governing equations for the system, Hamilton's principle is employed, necessitating the calculation of strain energy, kinetic energy, and the energy linked to external works. Displacement fields are defined as essential components of the mathematical formulation, and the hyperbolic beam theory is employed to describe the deformation behavior of the nanotube. Furthermore, the nonlocal strain gradient theory is coupled with the beam theory to account for size-dependent effects and derive the governing equations and boundary conditions.

2.2 Application of Hamilton's principle

The strain energy of the nanotube is expressed in terms of axial and shear deformations. Based on the hyperbolic beam theory, the axial strain 'ε_{ij}' and shear strain 'γ_{ij}' are related to the displacement fields. The strain energy 'S' is formulated as:

$$S = \frac{1}{2}\iiint (\sigma_{ij}\varepsilon_{ij} + \tau_{ij}\gamma_{ij})dV \tag{1}$$

where 'σ' is the stress tensor, and 'τ' is the shear stress tensor. The displacement fields along the 'x', 'y' and 'z' axis ($\bar{U}_1, \bar{U}_2,$ and $\bar{U}_3$) on the basis of the shear deformation hyperbolic beam theory are defined as follows:

$$\bar{U}_1 = u + \frac{(R_e - R_i)}{\pi} sinh\left(\frac{\pi z}{R_e - R_i}\right)\left(\phi + \frac{\partial w}{\partial x}\right) - z\left(\frac{\partial w}{\partial x}\right) \tag{2a}$$

$$\bar{U}_2 = 0 \tag{2b}$$

$$\bar{U}_1 = w(x,t) \tag{2c}$$

The axial, lateral and rotational components are shown by 'u', 'w' and 'ϕ'. Then, the stresses are calculated as follows:

$$\varepsilon_{xx} = \frac{\partial u}{\partial x} + \frac{R_e - R_i}{\pi} sinh\left(\frac{\pi z}{R_e - R_i}\right)\left(\frac{\partial \phi}{\partial x} + \frac{\partial^2 w}{\partial x^2}\right) - z\left(\frac{\partial^2 w}{\partial x^2}\right) \tag{3a}$$

$$\varepsilon_{xz} = \varepsilon_{zx} = \frac{1}{2} cosh\left(\frac{\pi z}{R_e - R_i}\right)\left(\phi + \frac{\partial w}{\partial x}\right) \tag{3b}$$

$$\varepsilon_{xy} = \varepsilon_{yy} = \varepsilon_{yx} = \varepsilon_{yz} = \varepsilon_{zz} = \varepsilon_{zy} = 0 \tag{3c}$$

The strain energy based on hyperbolic beam theory is calculated as follows:

$$S = \iiint \frac{1}{2}(\sigma_{xx}\varepsilon_{xx} + \tau_{xz}\gamma_{xz})dV = \iiint \bar{s}dV \tag{4a}$$

$$\begin{aligned}\bar{s} = {} & \frac{Ez^2}{2}\left(\frac{\partial^2 w}{\partial x^2}\right)^2 + \frac{G}{4} cosh\left(\frac{\pi z}{R_e - R_i}\right)^2 \left(\phi + \frac{\partial w}{\partial x}\right)^2 \\ & - \frac{ER_eR_i}{\pi^2} sinh\left(\frac{\pi z}{R_e - R_i}\right)^2 \left[\left(\frac{\partial \phi}{\partial x}\right)^2 + 2\frac{\partial \phi}{\partial x}\frac{\partial^2 w}{\partial x^2} + \left(\frac{\partial^2 w}{\partial x^2}\right)^2\right] \\ & + \frac{E(R_e - R_i)}{\pi} sinh\left(\frac{\pi z}{R_e - R_i}\right)\left(\frac{\partial u}{\partial x}\right)\left(\frac{\partial \phi}{\partial x} + \frac{\partial^2 w}{\partial x^2}\right) \\ & - \frac{Ez(R_e - R_i)}{\pi} sinh\left(\frac{\pi z}{R_e - R_i}\right)\left(\frac{\partial^2 w}{\partial x^2}\right)^2 - Ez\left(\frac{\partial u}{\partial x}\right)\left(\frac{\partial^2 w}{\partial x^2}\right) \\ & - \frac{Ez(R_e - R_i)}{\pi} sinh\left(\frac{\pi z}{R_e - R_i}\right)\left(\frac{\partial \phi}{\partial x}\right)\left(\frac{\partial^2 w}{\partial x^2}\right) + \frac{E}{2}\left(\frac{\partial u}{\partial x}\right)^2 + \\ & \frac{E\left(R_e^2 + {R_i}^2\right)}{2\pi^2} sinh\left(\frac{\pi z}{R_e - R_i}\right)^2 \left[\left(\frac{\partial \phi}{\partial x}\right)^2 + 2\frac{\partial \phi}{\partial x}\frac{\partial^2 w}{\partial x^2} + \left(\frac{\partial^2 w}{\partial x^2}\right)^2\right]\end{aligned} \tag{4b}$$

where 'E' is the elastic modulus. In the following, the Kinetic energy (K) based on the hyperbolic beam theory, is calculated as follows:

$$K = \frac{1}{2}\iiint \rho\left[\left(\frac{\partial \bar{U}_1}{\partial t}\right)^2 + \left(\frac{\partial \bar{U}_3}{\partial t}\right)^2\right]dV = \iiint \bar{K}dV \tag{5a}$$

$$\begin{aligned}\bar{K} = {} & -\frac{\rho z(R_e - R_i)}{\pi} sinh\left(\frac{\pi z}{R_e - R_i}\right)\left(\frac{\partial^2 w}{\partial x \partial t}\right)\left(\frac{\partial \phi}{\partial t} + \frac{\partial^2 w}{\partial x \partial t}\right) \\ & + \frac{\rho\left({R_e}^2 - 2R_eR_i + {R_i}^2\right)}{2\pi^2} sinh\left(\frac{\pi z}{R_e - R_i}\right)^2 \left(\frac{\partial \phi}{\partial t} + \frac{\partial^2 w}{\partial x \partial t}\right)^2 \\ & + \frac{\rho}{2}\left(\frac{\partial u}{\partial t}\right)^2 - \rho z\left(\frac{\partial u}{\partial t}\right)\left(\frac{\partial^2 w}{\partial x \partial t}\right) + \frac{\rho}{2}\left(\frac{\partial w}{\partial t}\right)^2 + \frac{\rho z^2}{2}\left(\frac{\partial^2 w}{\partial x \partial t}\right)^2 \\ & + \frac{\rho(R_e - R_i)}{\pi} sinh\left(\frac{\pi z}{R_e - R_i}\right)\left(\frac{\partial u}{\partial t}\right)\left(\frac{\partial \phi}{\partial t} + \frac{\partial^2 w}{\partial x \partial t}\right)\end{aligned} \tag{5b}$$

where 'ρ' is density. Also, the virtual energy of the external work ($\delta(W_E)$), which is the rotation force, is calculated as follows:

$$\delta(W_E) = -\frac{\partial}{\partial x}\left(\bar{F}_R \frac{\partial w}{\partial x}\right) + \bar{F}_R \frac{\partial w}{\partial x}\Big|_0^L \delta(w) \tag{6a}$$

$$\bar{F}_R = \int_x^L \int_A \rho\varpi^2(\zeta + x)dAdx \tag{6b}$$

where 'ϖ' is the rotational speed or angular velocity, and 'ς' is hub radius (hub radii). Hamilton's principle asserts that the change in the total energy functional with respect to time must equal zero:

$$\int_{t_1}^{t_2} \delta H dt = \int_{t_1}^{t_2} \delta S + \delta W_E - \delta K dt = 0 \tag{7}$$

The nonlocal strain gradient theory has emerged as a vital framework for analyzing the behaviors of size-dependent nanostructures, where traditional continuum mechanics often falls short. This theory incorporates two key components: the nonlocal effect, which involves long-range atomic interactions, and the strain gradient effect, which considers the influence of higher-order deformation gradients due to material variability at the nanoscale. By integrating these aspects, the nonlocal strain gradient theory provides a more accurate representation of the mechanical properties of nanostructures, such as nanotubes, nanobeams, and nanoplates, under various loading conditions. For instance, it has successfully predicted the bending, buckling, and vibrational behaviors of functionally graded materials and graphene-reinforced composites. This simultaneous analysis of nonlocality and strain gradients ensures that the model captures both softening effects (resulting from nonlocal interactions) and stiffening effects (due to strain gradients), offering a comprehensive framework for studying nanostructures in fields ranging from biomedical engineering to sports science. According to the nonlocal strain gradient theory, the stress-strain relationships are reformed as follows:

$$\sigma_{xx} - (ea)^2\nabla^2\sigma_{xx} = E{:}\,\varepsilon_{xx} - l^2\nabla^2(E{:}\,\varepsilon_{xx}) \tag{8a}$$

$$\tau_{xz} - (ea)^2\nabla^2\tau_{xz} = E{:}\,\gamma_{xz} - l^2\nabla^2(E{:}\,\gamma_{xz}) \tag{8b}$$

where 'ea' is the nonlocal parameter as well as 'l' is the strain gradient parameter.

2.3 Governing equations and boundary conditions

The governing equations and corresponding boundary conditions will be derived by employing the nonlocal strain gradient theory in conjunction with Hamilton's principle and utilizing the Euler-Lagrange principle.

'$\delta(u)$'

$$-l^2\Omega_1\frac{\partial^4 u}{\partial x^4} + \Omega_1\frac{\partial^2 u}{\partial x^2} = \Upsilon_1\frac{\partial^2 u}{\partial t^2} - (ea)^2\Upsilon_1\frac{\partial^4 u}{\partial x^2\partial t^2} \tag{9a}$$

'$\delta(\phi)$'

$$\begin{aligned}&l^2\Omega_2\left(\frac{\partial^3 w}{\partial x^3} + \frac{\partial^2\phi}{\partial x^2}\right) - \Omega_3\frac{\partial^3 w}{\partial x^3} + \Omega_4\left(\frac{\partial^3 w}{\partial x^3} + \frac{\partial^2\phi}{\partial x^2}\right)\\ &-\Omega_2\left(\frac{\partial w}{\partial x} + \phi\right) + l^2\Omega_3\frac{\partial^5 w}{\partial x^5} - l^2\Omega_4\left(\frac{\partial^5 w}{\partial x^5} + \frac{\partial^4\phi}{\partial x^4}\right) =\\ &\Upsilon_2\frac{\partial^2\phi}{\partial t^2} - \Upsilon_2(ea)^2\left(\frac{\partial^4\phi}{\partial x^2\partial t^2} + \Upsilon_3\frac{\partial^5 w}{\partial x^3\partial t^2}\right) - \Upsilon_3\frac{\partial^3 w}{\partial x\partial t^2}\end{aligned} \tag{9b}$$

'$\delta(w)$'

$$\begin{aligned}&-\Omega_2\left(\frac{\partial^2 w}{\partial x^2} + \frac{\partial\phi}{\partial x}\right) - \Omega_3\frac{\partial^3\phi}{\partial x^3} + l^2\Omega_2\left(\frac{\partial^4 w}{\partial x^4} + \frac{\partial^3\phi}{\partial x^3}\right)\\ &+\bar{F}_R\frac{\partial^2 w}{\partial x^2} + l^2\Omega_3\frac{\partial^5\phi}{\partial x^5} + l^2\Omega_5\frac{\partial^6 w}{\partial x^6} - \Omega_5\frac{\partial^4 w}{\partial x^4}\\ &+3(ea)^2\frac{d\bar{F}_R}{dx}\frac{\partial^3 w}{\partial x^3} + (ea)^2\bar{F}_R\frac{\partial^4 w}{\partial x^4} + (ea)^2\frac{d^3\bar{F}_R}{dx^3}\frac{\partial w}{\partial x}\\ &+3(ea)^2\frac{d^2\bar{F}_R}{dx^2}\frac{\partial^2 w}{\partial x^2} - \frac{d\bar{F}_R}{dx}\frac{\partial w}{\partial x}\\ &= (ea)^2\Upsilon_1\frac{\partial^4 w}{\partial x^2\partial t^2} + (ea)^2\Upsilon_3\frac{\partial^5\phi}{\partial x^3\partial t^2}\\ &+(ea)^2\Upsilon_4\frac{\partial^6 w}{\partial x^4\partial t^2} - \Upsilon_1\frac{\partial^2 w}{\partial t^2} - \Upsilon_3\frac{\partial^3\phi}{\partial x\partial t^2} - \Upsilon_4\frac{\partial^4 w}{\partial x^2\partial t^2}\end{aligned} \tag{9c}$$

Also, the boundary conditions are:
For the clamped type ($x = 0$):

$$u = 0, \phi = 0, w = 0 \tag{10a}$$

For the free type ($x = L$):

$$-l^2\Omega_1\frac{\partial^3 u}{\partial x^3} + \Omega_1\frac{\partial u}{\partial x} = (ea)^2\Upsilon_1\frac{\partial^3 u}{\partial x\partial t^2} \tag{10b}$$

$$\begin{aligned}&-l^2\Omega_4\left(\frac{\partial^4 w}{\partial x^4} + \frac{\partial^3\phi}{\partial x^3}\right) - \Omega_3\frac{\partial^2 w}{\partial x^2} + \Omega_4\left(\frac{\partial^2 w}{\partial x^2} + \frac{\partial\phi}{\partial x}\right) +\\ &l^2\Omega_3\frac{\partial^4 w}{\partial x^4} + (ea)^2\Upsilon_2\left(\frac{\partial^3\phi}{\partial x\partial t^2}\right) - \Upsilon_3(ea)^2\frac{\partial^4 w}{\partial x^2\partial t^2} = 0\end{aligned} \tag{10c}$$

$$\begin{aligned}&-\Omega_5\frac{\partial^2 w}{\partial x^2} - \Omega_3\frac{\partial\phi}{\partial x} + l^2\Omega_5\frac{\partial^4 w}{\partial x^4} + \Omega_3\frac{\partial^3\phi}{\partial x^3}\\ &+(ea)^2\left(\Upsilon_1\frac{\partial^3 w}{\partial x\partial t^2} + \Upsilon_3\frac{\partial^3\phi}{\partial x\partial t^2} + \Upsilon_4\frac{\partial^4 w}{\partial x^2\partial t^2}\right) = 0\end{aligned} \tag{10d}$$

$$\begin{aligned}&\Omega_5\frac{\partial^3 w}{\partial x^3} - l^2\Omega_3\frac{\partial^4\phi}{\partial x^4} - l^2\Omega_5\frac{\partial^5 w}{\partial x^5} - (ea)^2\bar{F}_R\frac{\partial^2 w}{\partial x^2}\bar{F}_R\frac{\partial w}{\partial x}\\ &+\Omega_3\frac{\partial^2\phi}{\partial x^2} + (ea)^2\left(\Upsilon_4\frac{\partial^5 w}{\partial x^3\partial t^2} + \Upsilon_3\frac{\partial^4\phi}{\partial x^2\partial t^2} + \Upsilon_1\frac{\partial^3 w}{\partial x\partial t^2}\right)\\ &-(ea)^2\frac{d\bar{F}_R}{dx}\frac{\partial w}{\partial x} - l^2\Omega_2\left(\frac{\partial^3 w}{\partial x^3} + \frac{\partial^2\phi}{\partial x^2}\right) + \Omega_2\left(\frac{\partial w}{\partial x} + \phi\right) = 0\end{aligned} \tag{10e}$$

where

$$\Omega_1 = \iint E r dr d\theta \tag{11a}$$

$$\Omega_2 = \iint GK_S\cosh\left(\frac{\pi r\sin(\theta)}{R_e - R_i}\right)^2 r dr d\theta \tag{11b}$$

$$\begin{aligned}\Omega_3 = &-\iint E\frac{(R_e - R_i)^2}{\pi^2}\sinh\left(\frac{\pi r\sin(\theta)}{R_e - R_i}\right)^2 r dr d\theta\\ &+\iint E\frac{(R_e - R_i)}{\pi} r\sin(\theta)\sinh\left(\frac{\pi r\sin(\theta)}{R_e - R_i}\right) r dr d\theta\end{aligned} \tag{11c}$$

$$\Omega_4 = \iint E\frac{(R_e - R_i)}{\pi}\sin(\theta)\sinh\left(\frac{\pi r\sin(\theta)}{R_e - R_i}\right) r^2 dr d\theta \tag{11d}$$

$$\begin{aligned}\Omega_5 = &-\iint E\frac{(R_e - R_i)^2}{\pi^2}\sinh\left(\frac{\pi r\sin(\theta)}{R_e - R_i}\right)^2 r dr d\theta\\ &+2\iint E\frac{(R_e - R_i)}{\pi} r\sin(\theta)\sinh\left(\frac{\pi r\sin(\theta)}{R_e - R_i}\right) r dr d\theta\end{aligned} \tag{11e}$$

$$-\iint Er^3\sin^2(\theta)\,drd\theta$$

$$\Upsilon_1 = \iint \rho r dr d\theta \tag{11f}$$

$$\Upsilon_2 = \iint \rho\frac{(R_e-R_i)^2}{\pi^2}sinh\left(\frac{\pi r sin(\theta)}{R_e-R_i}\right)^2 r dr d\theta \tag{11g}$$

$$\begin{aligned}\Upsilon_3 = &-\iint \rho\frac{(R_e-R_i)^2}{\pi^2}sinh\left(\frac{\pi r sin(\theta)}{R_e-R_i}\right)^2 r dr d\theta\\ &+\iint \rho\frac{(R_e-R_i)}{\pi} r\sin(\theta)\sinh\left(\frac{\pi r\sin(\theta)}{R_e-R_i}\right) r dr d\theta\end{aligned} \tag{11h}$$

$$\begin{aligned}\Upsilon_4 = &-\iint \rho\frac{(R_e-R_i)^2}{\pi^2}sinh\left(\frac{\pi r sin(\theta)}{R_e-R_i}\right)^2 r dr d\theta\\ &+2\iint \rho\frac{(R_e-R_i)}{\pi} r\sin(\theta)\sinh\left(\frac{\pi r\sin(\theta)}{R_e-R_i}\right) r dr d\theta\\ &-\iint \rho r^3\sin^2(\theta)\,drd\theta\end{aligned} \tag{11i}$$

where 'K_S' is the shear correction factor.

3. Numerical methodology for solving governing equations

The Finite Element Method (FEM) is utilized to address the governing equations established for the rotating nanotube, which integrates hyperbolic higher-order beam theory alongside nonlocal strain gradient theory. FEM is chosen for its adaptability in managing intricate geometries, nonlinearities, and boundary conditions, while also addressing size-dependent effects essential to nanoscale systems. The process consists of breaking the nanotube into finite elements, formulating the weak form of the governing equations, and iteratively solving the resulting system of equations. The governing equations are cast into their weak form by multiplying with test functions and integrating over the nanotube domain. The weak forms for the axial displacement 'u', rotational angle 'ϕ', and transverse displacement 'w' are:

Axial Weak Form:

$$\int\begin{bmatrix}-l^2\Omega_1\dfrac{\partial^4 u}{\partial x^4}+\Omega_1\dfrac{\partial^2 u}{\partial x^2}\\ -\Upsilon_1\dfrac{\partial^2 u}{\partial t^2}+(ea)^2\Upsilon_1\dfrac{\partial^4 u}{\partial x^2\partial t^2}\end{bmatrix}\delta(u)dx = 0 \tag{12a}$$

Rotational Weak Form:

$$\int\begin{bmatrix}l^2\Omega_2\left(\dfrac{\partial^3 w}{\partial x^3}+\dfrac{\partial^2\phi}{\partial x^2}\right)+\Omega_4\left(\dfrac{\partial^3 w}{\partial x^3}+\dfrac{\partial^2\phi}{\partial x^2}\right)\\ -\Omega_2\left(\dfrac{\partial w}{\partial x}+\phi\right)+l^2\Omega_3\dfrac{\partial^5 w}{\partial x^5}\\ +\Upsilon_2(ea)^2\left(\dfrac{\partial^4\phi}{\partial x^2\partial t^2}+\Upsilon_3\dfrac{\partial^5 w}{\partial x^3\partial t^2}\right)\\ +\Upsilon_3\dfrac{\partial^3 w}{\partial x\partial t^2}-l^2\Omega_4\left(\dfrac{\partial^5 w}{\partial x^5}+\dfrac{\partial^4\phi}{\partial x^4}\right)\\ -\Upsilon_2\dfrac{\partial^2\phi}{\partial t^2}-\Omega_3\dfrac{\partial^3 w}{\partial x^3}\end{bmatrix}\delta\phi dx = 0 \tag{12b}$$

Transverse Weak Form:

$$\int\begin{bmatrix}-\Omega_2\left(\dfrac{\partial^2 w}{\partial x^2}+\dfrac{\partial\phi}{\partial x}\right)-\Omega_3\dfrac{\partial^3\phi}{\partial x^3}+\bar{F}_R\dfrac{\partial^2 w}{\partial x^2}\\ +l^2\Omega_2\left(\dfrac{\partial^4 w}{\partial x^4}+\dfrac{\partial^3\phi}{\partial x^3}\right)-(ea)^2\Upsilon_4\dfrac{\partial^6 w}{\partial x^4\partial t^2}\\ +l^2\Omega_3\dfrac{\partial^5\phi}{\partial x^5}+l^2\Omega_5\dfrac{\partial^6 w}{\partial x^6}-\Omega_5\dfrac{\partial^4 w}{\partial x^4}\\ +3(ea)^2\dfrac{d\bar{F}_R}{dx}\dfrac{\partial^3 w}{\partial x^3}+3(ea)^2\dfrac{d^2\bar{F}_R}{dx^2}\dfrac{\partial^2 w}{\partial x^2}\\ +(ea)^2\bar{F}_R\dfrac{\partial^4 w}{\partial x^4}+(ea)^2\dfrac{d^3\bar{F}_R}{dx^3}\dfrac{\partial w}{\partial x}\\ +\Upsilon_4\dfrac{\partial^4 w}{\partial x^2\partial t^2}-\dfrac{d\bar{F}_R}{dx}\dfrac{\partial w}{\partial x}-(ea)^2\Upsilon_1\dfrac{\partial^4 w}{\partial x^2\partial t^2}\\ -(ea)^2\Upsilon_3\dfrac{\partial^5\phi}{\partial x^3\partial t^2}+\Upsilon_1\dfrac{\partial^2 w}{\partial t^2}+\Upsilon_3\dfrac{\partial^3\phi}{\partial x\partial t^2}\end{bmatrix}\delta w dx \tag{12c}$$

The nanotube is divided into 'N' finite elements, with Hermitian shape functions '$N_i(x)$' used to approximate 'u', 'w', and 'ϕ':

$$u(x,t)\approx\sum_{i=1}^{n}N_i(x)u_i(t) \tag{13a}$$

$$w(x,t)\approx\sum_{i=1}^{n}N_i(x)w_i(t) \tag{13b}$$

$$\phi(x,t)\approx\sum_{i=1}^{n}N_i(x)\phi_i(t) \tag{13c}$$

This guarantees consistent displacements and rotations throughout the elements. Next, the Newmark-beta method is utilized to estimate time derivatives, guaranteeing unconditional stability in dynamic issues:

$$\frac{\partial^2 u}{\partial x^2}\approx\frac{u^{n+1}-u^n}{\Delta t^2},\frac{\partial w}{\partial x}\approx\frac{w^{n+1}-w^n}{\Delta t} \tag{14}$$

The weak forms are divided to create the global stiffness (K) and mass (M) matrices:

$$M\ddot{U}+KU=0 \tag{15}$$

In which '$U=\{u,w,\phi\}^T$'. This formulation facilitates the examination of stability, resonance, and dynamic responses under exercise-induced hemodynamic conditions, essential for enhancing the performance of nanodevices in drug delivery systems. The numerical framework based on FEM adeptly accounts for the intertwined impacts of rotational dynamics, size-dependent nonlocal strain gradients, and hemodynamic forces on the stability of nanotubes. This strategy offers a solid foundation for creating dependable nanodevices in dynamic physiological settings.

4. Presentation of numerical results

This section presents quantitative results aimed at connecting sophisticated engineering simulations in the field of bioengineering, with a particular emphasis on enhanced drug delivery systems utilizing nanotechnology.

Table 1 Validation of numerical results for the natural frequencies of the system under various nonlocal parameters (ea) and angular velocities (ϖ)

	$(ea)^2$=0	$(ea)^2 = 2L$	$(ea)^2 = 4L$
Liu *et al*. (2022), Third-order beam theory			
$\varpi = 0$	1.9837	1.99058	2.01202
$\varpi = 2\sqrt{2EI/L^4\rho A}$	2.63655	2.68144	2.82311
$\varpi = 4\sqrt{2EI/L^4\rho A}$	3.9741	4.08093	4.43747
$\varpi = 6\sqrt{2EI/L^4\rho A}$	5.48721	5.66021	6.26151
$\varpi = 8\sqrt{2EI/L^4\rho A}$	7.04856	7.29542	8.1598
Current results, Hyperbolic beam theory			
$\varpi = 0$	1.985684	1.993367	2.014434
$\varpi = 2\sqrt{2EI/L^4\rho A}$	2.63945	2.684926	2.82678

This study seeks to assess the efficacy and reliability of nano-devices in the delivery of therapeutic agents across various external and physiological conditions. Specifically, the study will examine the impact of physical exercise on these systems. The distribution, retention, and efficacy of drug-delivery mechanisms can be substantially impacted by the dynamic changes in blood flow, tissue deformation, and mechanical loading that physical activity induces. We simulate the interaction between the behavior of nano-devices within biological environments and exercise-induced biomechanical factors by utilizing robust computational models and numerical methodologies. These simulations not only offer critical insights into the optimization of drug-delivery systems but also emphasize the significance of integrating mechanical engineering principles with biomedical sciences to develop more effective and adaptive therapeutic solutions. The findings presented in this article will clarify the role of exercise as a critical modulator in improving drug-delivery outcomes, thereby facilitating the development of personalized and activity-aware medical interventions.

To validate the numerical results for both the solution methodology and the derivation of governing equations, a careful comparison is required between the current results obtained through Hyperbolic Beam Theory and those reported by Liu *et al*. (2022) using Third-Order Beam Theory. This comparison validates the precision and dependability of the governing equations and the used numerical techniques. Before addressing new results, validating the numerical solution methods and the governing equations is essential. Table 1 compares the results from this study, which employs Hyperbolic Beam Theory, with those reported by Liu *et al*. (2022) who utilized Third-Order Beam Theory. Validation is conducted for multiple values of the nonlocal parameter (ea) and varying levels of angular velocity (ϖ). The validation in Table 1 confirms the accuracy and reliability of the numerical solution method and the governing equations. The current method's reliability is highlighted by its alignment with benchmark results from Liu *et al*. (2022) facilitating further investigations into advanced applications in nanotechnology and bioengineering. Before presenting new findings, it is essential to undertake a validation step to ensure that the conclusions are based on a robust foundation of known procedures and equations.

The mechanical properties of carbon nanotubes (CNTs) are crucial in influencing their performance across diverse engineering applications, such as nano-scale drug delivery devices. Carbon nanotubes demonstrate remarkable material properties, including a high elastic modulus (E), low density (ρ), and a defined Poisson's ratio (ν), rendering them suitable for improving structural stability and dynamic response (Dai *et al*. 2021, Li *et al*. 2022). The elastic modulus of carbon nanotubes (CNTs) generally varies from 1 to $5\,TPa$, influenced by factors such as chirality and diameter, with a density of approximately $1.3-2.1\ g/cm^3$, which is considerably lower than that of most conventional materials (Lekawa-Raus *et al*. 2014). The Poisson's ratio of carbon nanotubes (CNTs) is typically reported to range from 0.19 to 0.25, indicating their distinct anisotropic properties (Wang *et al*. 2019). The mechanical properties were employed in this analysis to compute the results, ensuring that the derived outcomes are founded on accurate and reliable material characteristics. The computational framework utilizes these properties to effectively represent the system's behavior across different conditions, thus confirming the accuracy of the results.

A set of non-dimensional parameters has been introduced to enhance the interpretation and presentation of the results. The parameters facilitate a generalized analysis by removing dependencies on particular material or geometric properties, thus improving the scalability and applicability of the results. With 'ω' standing for the natural frequency, 'L' for the structure's length, 'R_e' for the external tube radius, 'ρ' for the density, A for the cross-sectional area, and 'E' and 'I' for the Young's modulus and moment of inertia, respectively, the dimensionless frequency is defined as '$\sqrt{\omega\, L^2/R_e \sqrt{\rho A/\pi EI}}$'. The dimensionless rotating speed is expressed as '$\Lambda = \varpi\, \pi/L^2 \sqrt{EI/\rho A}$', indicating the influence of angular velocity on the system's dynamics. The dimensionless hub radii, represented as '$\frac{\zeta}{L}$', provide an understanding of the hub's size relative to the total length of the structure. While the dimensionless nonlocal parameter, '$\frac{2ea}{\pi L}$', indicates the scale effects caused by nonlocal elasticity theory, the dimensionless strain gradient parameter, '$\frac{l}{R_e}$'l, shows the influence of higher-order continuum theories on mechanical response. The non-dimensional parameters provide a normalized representation of the results to facilitate direct comparisons across different setups and enhance comprehension of the underlying mechanics.

The numerical results are summarized in this part, which also connects the observed phenomena to the stability of nanodevices used in exercise-influenced drug delivery applications. The influence of strain gradient, hub radii, rotational velocity, and nonlocal factors on the dynamic behavior of nanotubes is discussed here, with clear implications for improving their performance in physiological settings. The results show a direct correlation between angular velocity (Λ) and dimensionless frequency (see Table 2 and Fig. 3). The influence of angular velocity and

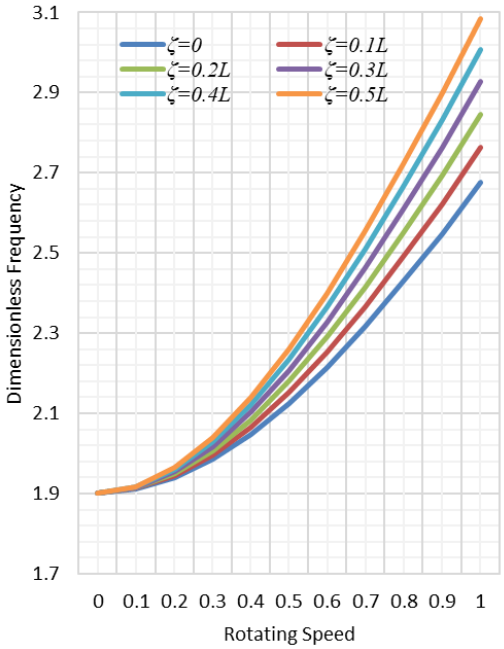

Fig. 3 Influence of angular velocity (Λ) and hub radii (ζ) on the dimensionless frequency ($\sqrt{\omega {L^2}/{R_e}\sqrt{\rho A/\pi EI}}$) of a rotating nanotube, '$L = 15R_e$', '$R_e = 0.99R_i$'

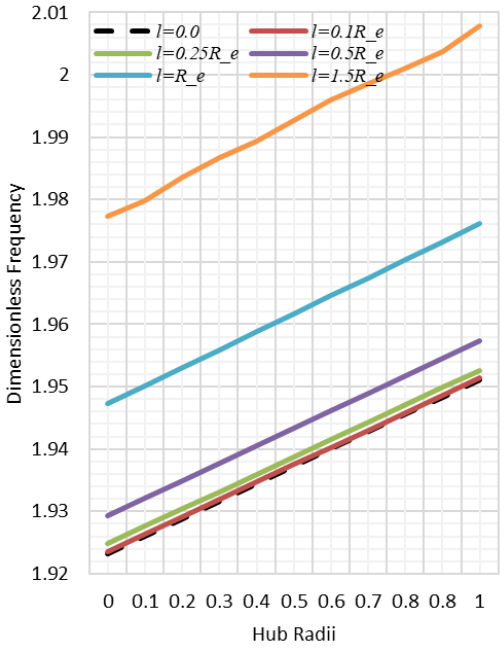

Fig. 4 Effect of the strain gradient parameter (l) and hub radii (ζ) on the dimensionless frequency ($\sqrt{\omega {L^2}/{R_e}\sqrt{\rho A/\pi EI}}$) of a nanotube, '$\varpi\pi\sqrt{EI/\rho A} = 0.15L^2$', '$L = 15R_e$', '$R_e = 0.99R_i$'

radius ratio (R_e/R_i) on the dimensionless frequency ($\sqrt{\omega {L^2}/{R_e}\sqrt{\rho A/\pi EI}}$) of a cantilevered nanotube is analyzed in Table 2. As 'Λ' increases, the frequency increases due to centrifugal stiffening, a phenomenon in which rotational motion generates radial stresses that augment structural rigidity. At '$R_e/R_i = 0.95$', the frequency increases by 45.5% as 'Λ' increases from 0.0 to 1.0. Increasing the radius ratio, which corresponds to thinner nanotube walls, results in a reduction of frequency, as a higher 'R_e/R_i' diminishes the flexural stiffness of the structure. The results highlight that in the construction of nanodevices, it is essential to equilibrate wall thickness and rotation speed to provide stability amid exercise-induced hemodynamic fluctuations, including increased blood flow velocities. Fig. 3 illustrates the cumulative effect of hub radii (ζ) and rotational velocity on the dimensionless frequency of the nanotube. Larger hub radii amplify centrifugal forces at the fixed end, increasing structural stiffness and raising frequencies. At '$\Lambda = 1.0$', the frequency increases by 57.5% as 'ζ' rises from 0 to 0.5L. This trend aligns with the principle that rotational inertia and geometric constraints dominate dynamic stability. In drug delivery systems, where hub shape has to be tailored to withstand the mechanical stresses brought on by physical activity, such insights are essential for building nanomotors. The rotational dynamics of nanodevices in areas with high blood flow, such as arteries, during physical activity are simulated by increased angular velocities. By improving stability, the frequency increase avoids resonance-related failure. The ability to deliver drugs may be compromised by excessive wall thinning ($R_e/R_i \to 1$), which calls for material reinforcements such graphene origami.

Dimensionless frequency ($\sqrt{\omega {L^2}/{R_e}\sqrt{\rho A/\pi EI}}$)
Dimensionless rotating speed ($\varpi {\pi}/{L^2}\sqrt{EI/\rho A}$)
Dimensionless hub radii (ζ/L)
Dimensionless nonlocal parameter ($\frac{2ea}{\Pi L}$)
Dimensionless strain gradient parameter ($\frac{l}{R_e}$)

Fig. 4 examines the interplay between the strain gradient parameter (l) and hub radii (ζ). The strain gradient parameter introduces size-dependent stiffening, elevating frequencies as 'l/R_e' increases. For '$\zeta = 0.5L$', the frequency rises by 22.8% when 'l/R_e' increases from 0 to 1.5. The stiffening effect and alterations in hub radii demonstrate the potential for optimizing geometric design and material heterogeneity to enhance the stability of nanodevices in dynamic environments. The necessity for nanodevices to maintain structural integrity during intense physical activity renders these findings particularly relevant for applications in sports medicine. Strain gradient stiffening reduces the probability of deformation in high-stress areas, such as joints, during physical activity. Under mechanically challenging conditions, the ability of nanodevices to maintain stability while demonstrating flexibility enables regulated drug administration.

Fig. 5A and 5B illustrate the effects of the nonlocal parameter (ea) under local and nonlocal boundary conditions (BCs). The asymmetric constraints of a cantilever nanotube, with one end fixed and the other free, amplify the sensitivity of the free end to nonlocal effects due to the lack of counteracting constraints. In symmetrically constrained systems (e.g., clamped-clamped), stresses are

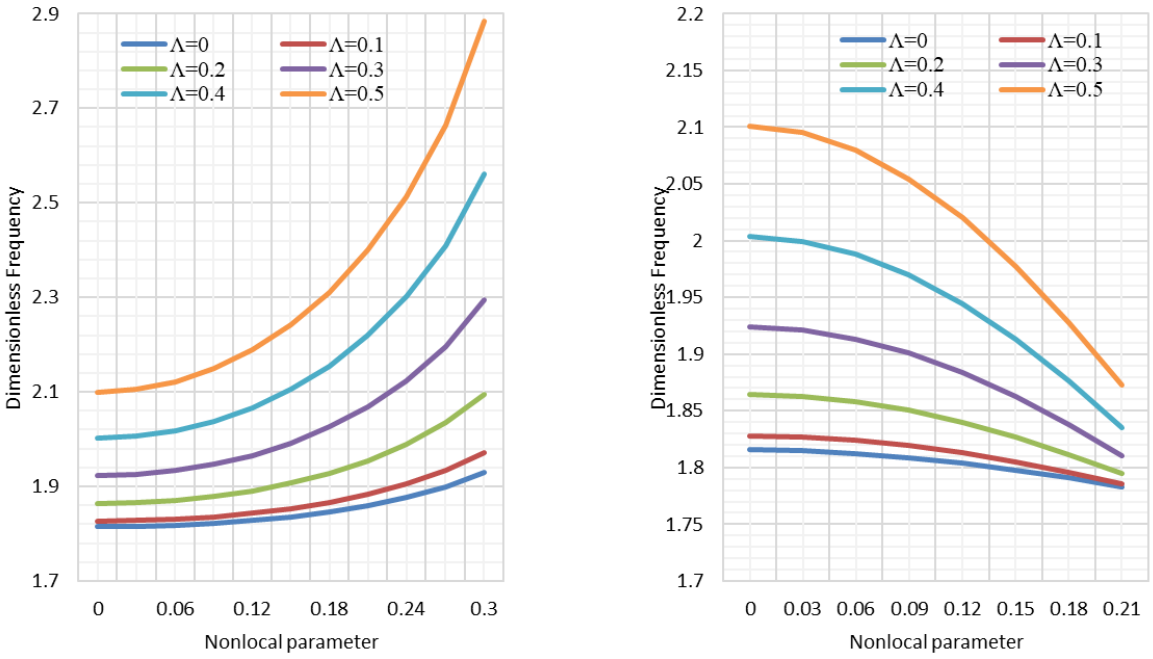

A: Local boundary conditions: B: Non-local boundary conditions:

Fig. 5 Dual response of the nonlocal parameter $(2ea/\pi L)$ under (A) local and (B) nonlocal boundary conditions for varying Λ, '$l = R_e$', '$\varsigma = 0.22L$', '$L = 10R_e$', '$R_e = 0.98R_i$'

Table 2 Dimensionless frequency $(\sqrt{\omega {L^2}/{R_e}\sqrt{\rho A/\pi EI}})$ of a rotating cantilever nanotube under varing angular velocities ($\Lambda = \varpi {\pi}/{L^2}\sqrt{EI/\rho A}$) (Λ) and radius ratios (R_e/R_i)., '$L = 15R_e$', '$\zeta = 0.1L$'

Angular Velocity	$R_e/R_i = 0.95$	$R_e/R_i = 0.96$	$R_e/R_i = 0.97$	$R_e/R_i = 0.98$	$R_e/R_i = 0.99$	$R_e/R_i = 0.999$
$\Lambda = 0.0$	1.938246036	1.904353307	1.903606871	1.902853576	1.90209345	1.901403518
$\Lambda = 0.1$	1.948922733	1.915052698	1.914306889	1.913554233	1.912794756	1.91210542
$\Lambda = 0.2$	1.980588054	1.946774242	1.94603005	1.945279043	1.944521248	1.943833452
$\Lambda = 0.3$	2.032204938	1.99844862	1.997706317	1.996957245	1.99620143	1.995515456
$\Lambda = 0.4$	2.102216116	2.068474231	2.067733111	2.06698527	2.066230737	2.06554596
$\Lambda = 0.5$	2.188743216	2.15492616	2.1541845	2.153436163	2.15268118	2.151996038
$\Lambda = 0.6$	2.289781702	2.255759176	2.255014385	2.254262949	2.253504901	2.252817032
$\Lambda = 0.7$	2.403356815	2.368968419	2.368217288	2.367459528	2.366695175	2.366001649
$\Lambda = 0.8$	2.527627848	2.492695214	2.491934195	2.491166547	2.490392309	2.48968989
$\Lambda = 0.9$	2.660944604	2.625282849	2.624508317	2.623727142	2.622939365	2.622224754
$\Lambda = 1.0$	2.801867705	2.765295056	2.764503523	2.763705321	2.762900493	2.762170522

distributed more uniformly, leading nonlocal effects to produce predictable softening typically. The unconstrained free end in cantilevers allows nonlocal interactions to dominate their mechanical response. Under local boundary conditions, the nonlocal parameter $(2ea/\pi L)$ enhances the bulk material, increasing natural frequencies by improving resistance to bending. Conversely, atomic-scale interactions at the fixed end distribute stresses under nonlocal boundary conditions, softening the structure and reducing frequencies. The continual rise in frequency with 'Λ' across all instances (reaching 53.5% at $\Lambda = 1.0$) underscores the preeminence of rotational dynamics in stabilizing nanodevices during operation. This dichotomy underscores the importance of choosing boundary conditions in the simulation of physiological environments. Local boundary conditions simulate confined areas, like capillaries, whereas nonlocal boundary conditions characterize open systems, such as arteries. In open systems, nonlocal effects dominate during exercise due to the dynamic interactions of blood flow. Designers must account for these effects to prevent frequency alterations that could destabilize nanodevices or trigger unintended medication release.

This phenomenon is crucial for drug delivery design since nanodevices often operate within dynamic physiological settings characterized by variable constraints. In restricted environments, such as capillaries, localized

boundary conditions, and rigidity effects maintain stability against turbulence in blood flow during physical exertion. Nonlocal boundary conditions and softening effects provide adaptive flexibility for handling intricate hemodynamic stresses in open systems such as arteries. Comprehending this duality enables engineers to customize the materials and design of nanodevices for specific purposes, hence enhancing the stability and precision of targeted drug delivery. The findings underscore the significance of boundary conditions in biological applications and align with other studies on wave dispersion in poroelastic beams and graphene-reinforced nanomaterials.

5. Conclusions

The stability analysis of rotating cantilever nanotubes for drug delivery applications was conducted using a combination of hyperbolic higher-order beam theory and nonlocal strain gradient theory. Numerical solutions were obtained using the finite element method (FEMs). The results suggested that mechanical parameters, such as angular velocity, hub radii, nonlocal effects, and strain gradients substantially influence the dynamic behavior of nanodevices in exercise-mediated hemodynamic conditions.

Increased angular velocity raised natural frequencies due to centrifugal stiffening, thereby stabilizing nanodevices in high-blood-flow environments. Conversely, higher radius ratios decreased frequencies, requiring geometric optimization to achieve a balance between flexibility and rigidity. Larger hub radii increased rotational inertia, thereby improving stability, while strain gradient parameters introduced size-dependent stiffening essential for sustaining performance in heterogeneous biological tissues. The nonlocal parameter demonstrated a dual response: it exhibited stiffening under local boundary conditions and softening under nonlocal boundary conditions, which can be attributed to stress redistribution at the fixed end and the sensitivity of the free end to atomic-scale interactions. The results were validated against previous studies, confirming the accuracy of the computational framework. The interaction of nonlocal and strain gradient effects, along with rotational dynamics, establishes a basis for optimizing nanodevice designs for dynamic physiological conditions, facilitating dependable drug transport and regulated release during physical activity. Future research should investigate adaptive materials and machine learning algorithms to enhance real-time stability in vivo, integrating mechanical engineering principles with biomedical innovation for applications in sports medicine and personalized healthcare.

References

Afshari Behzad, M., Mirjavadi Seyed, S. and Barati Mohammad, R. (2022), "Investigating nonlinear static behavior of hyper-elastic plates using three-parameter hyperelastic model", *Adv. Concr. Constr.*, **13**(5), 377-384. https://doi.org/10.12989/ACC.2022.13.5.377.

Chen, F., Chen, J., Duan, R., Habibi, M. and Khadimallah, M.A. (2022), "Investigation on dynamic stability and aeroelastic characteristics of composite curved pipes with any yawed angle", *Compos. Struct.*, **284**, 115195. https://doi.org/10.1016/j.compstruct.2022.115195.

Dai, Z., Jiang, Z., Zhang, L. and Habibi, M. (2021), "Frequency characteristics and sensitivity analysis of a size-dependent laminated nanoshell", *Adv. Nano Res.*, **10**(2), 175-189. https://doi.org/10.12989/anr.2021.10.2.175.

Guo, Y., Maalla, A., Habibi, M. and moradi, Z. (2024), "Electroelastic wave dispersion in the rotary piezoelectric NEMS sensors/actuators via nonlocal strain gradient theory", *Mech. Syst. Signal Pr.*, **216**, 111453. https://doi.org/10.1016/j.ymssp.2024.111453.

Hao, X., Jiang, B., Wu, J., Xiang, D., Xiong, Z., Li, C., Li, Z., He, S., Tu, C. and Li, Z. (2024), "Nanomaterials for bone metastasis", *J. Control. Release*, **373**, 640-651. https://doi.org/10.1016/j.jconrel.2024.07.067.

He, L., Habibi, M. and Khorami, M. (2024), "Semi-analytical stability behavior of composite concrete structures via modified non-classical theories", *Adv. Concr. Constr.*, **17**(4), 187. https://doi.org/10.12989/acc.2024.17.4.187.

Huang, J., Pan, Z., Yang, S., Habibi, M. and Safa, M. (2024), "Bending-based solution methodology using eigenvalue-eigenvector approach for analysis of foldable reinforced Golf Clubs cylindrical shell", *Mech. Adv. Mater. Struct.*, 1-14. https://doi.org/10.1080/15376494.2024.2378372.

Huo, J., Zhang, G., Ghabussi, A. and Habibi, M. (2021), "Bending analysis of FG-GPLRC axisymmetric circular/annular sector plates by considering elastic foundation and horizontal friction force using 3D-poroelasticity theory", *Compos. Struct.*, **276**, 114438. https://doi.org/10.1016/j.compstruct.2021.114438.

Jia, S., Niu, X., Jia, F. and Mahmoudi, T. (2023), "Advantages and disadvantages of renewable energy-oil-environmental pollution-from the point of view of nanoscience", *Adv. Concr. Constr.*, **16**(1), 69-78. https://doi.org/10.12989/acc.2023.16.1.069.

Jin, Z., Huo, W., Habibi, M. and Albaijan, I. (2024), "Thermo-foldable bending analysis of tunable shells using a higher-order modeling", *Mech. Adv. Mater. Struct.*, 1-14. https://doi.org/10.1080/15376494.2024.2369263.

Kazemi, M., Nabavi, S., Gratuze, M. and Nabki, F. (2023), "Anchor loss reduction in micro-electro mechanical systems flexural beam resonators using trench hole array reflectors", *Micromachines*, **14**(11), 2036. https://doi.org/10.3390/mi14112036.

Kazemi, M., Nabavi, S., Gratuze, M. and Nabki, F. (2024), "Frequency selection in a MEMS flexural beam resonator by electrostatic actuation", *J. Microelectromech. Syst.*, **33**(1), 66-77. https://doi.org/10.1109/JMEMS.2023.3331701.

Lei, X., Li, Z., Zhong, Y., Li, S., Chen, J., Ke, Y., Lv, S., Huang, L., Pan, Q., Zhao, L., Yang, X., Chen, Z., Deng, Q. and Yu, X. (2022), "Gli1 promotes epithelial–mesenchymal transition and metastasis of non-small cell lung carcinoma by regulating snail transcriptional activity and stability", *Acta Pharmaceutica Sinica B*, **12**(10), 3877-3890. https://doi.org/10.1016/j.apsb.2022.05.024.

Lekawa-Raus, A., Kurzepa, L., Peng, X. and Koziol, K. (2014), "Towards the development of carbon nanotube based wires", *Carbon*, **68** 597-609. https://doi.org/10.1016/j.carbon.2013.11.039.

Li, J., Wu, Z., Habibi, M. and Albaijan, I. (2024a), "An inspection of the metal-foam beam considering torsional dynamic responses", *Solid State Commun.*, **391**, 115638. https://doi.org/10.1016/j.ssc.2024.115638.

Li, Y., Habibi, M. and Bagheri, M. (2024b), "AI-driven prediction of linear and nonlinear buckling in nonuniform functionally graded micro-tubes for sports equipment in sports training", *Adv. Nano Res.*, **17**(6), 559. https://doi.org/10.12989/anr.2024.17.6.559.

Li, Y., Li, S., Guo, K., Fang, X. and Habibi, M. (2022), "On the modeling of bending responses of graphene-reinforced higher order annular plate via two-dimensional continuum mechanics approach", *Eng. Comput.*, **38**(1), 703-724. https://doi.org/10.1007/s00366-020-01166-w.

Liang, Z., Zhao, Y., Yu, H., Habibi, M. and Mahmoudi, T. (2024), "Artificial neural networks coupled with numerical approach for the stability prediction of non-uniform functionally graded microscale cylindrical structures", *Structures*, **60**, 105826. https://doi.org/10.1016/j.istruc.2023.105826.

Liu, X., Zhang, X. and Habibi, M. (2024), "DNS key technologies based on machine learning and network data mining", *Adv. Concr. Constr.*, **17**(2), 53. https://doi.org/10.12989/acc.2024.17.2.053

Liu, Y., Wang, X., Li, L., Wu, B. and Yang, Q. (2022), "On the forced vibration of high-order functionally graded nanotubes under the rotation via intelligent modeling", *Adv. Nano Res.*, **13**(1), 47-61. https://doi.org/10.12989/anr.2022.13.1.047.

Ma, B., Chen, K.Y., Habibi, M. and Albaijan, I. (2024), "Static/ dynamic analyses of sandwich micro-plate based on modified strain gradient theory", *Mech. Adv. Mater. Struct.*, **31**(23), 5760-5767. https://doi.org/10.1080/15376494.2023.2219453.

Man, Y., Habibi, M. and Maleki, B. (2024), "Biodiesel synthesis from waste coconut scum oil utilizing SnFe2O4/cigarette butt-derived biochar as a magnetic nanocatalyst: Optimization, kinetic and thermodynamic study", *Chem. Eng. Res. Des.*, **210**, 311-327. https://doi.org/10.1016/j.cherd.2024.08.033.

Mirjavadi, S.S., Afshari, B.M., Barati, M.R. and Hamouda, A.M.S. (2020a), "Transient response of porous inhomogeneous nanobeams due to various impulsive loads based on nonlocal strain gradient elasticity", *Int. J. Mech. Mater. Des.*, **16**(1), 57-68. https://doi.org/10.1007/s10999-019-09452-2.

Mirjavadi, S.S., Forsat, M., Badnava, S. and Barati, M.R. (2020b), "Analyzing nonlocal nonlinear vibrations of two-phase geometrically imperfect piezo-magnetic beams considering piezoelectric reinforcement scheme", *J. Strain Anal. Eng. Des.*, **55**(7-8), 258-270. https://doi.org/10.1177/0309324720917285.

Mirjavadi, S.S., Forsat, M., Badnava, S., Barati, M.R. and Hamouda, A.M.S. (2020c), "Nonlinear dynamic characteristics of nonlocal multi-phase magneto-electro-elastic nano-tubes with different piezoelectric constituents", *Appl. Phys. A*, **126**(8), 605. https://doi.org/10.1007/s00339-020-03743-8.

Mirjavadi, S.S., Forsat, M., Barati, M.R. and Hamouda, A. (2020d), "Investigating nonlinear vibrations of multi-scale truncated conical shell segments with carbon nanotube/ fiberglass reinforcement using a higher order conical shell theory", *J. Strain Anal. Eng. Des.*, **56**(3), 181-192. https://doi.org/10.1177/0309324720939811.

Mirjavadi, S.S., Forsat, M., Barati, M.R. and Hamouda, A.M.S. (2022a), "Analysis of nonlinear vibrations of CNT- /fiberglass-reinforced multi-scale truncated conical shell segments", *Mech. Based Des. Struct.*, **50**(6), 2067-2083. https://doi.org/10.1080/15397734.2020.1768866.

Mirjavadi, S.S., Forsat, M., Barati, M.R. and Hamouda, A.M.S. (2022b), "Geometrically nonlinear vibration analysis of eccentrically stiffened porous functionally graded annular spherical shell segments", *Mech. Based Des. Struct.*, **50**(6), 2206-2220. https://doi.org/10.1080/15397734.2020.1771729.

Mirjavadi, S.S., Forsat, M., Barati, M.R. and Hamouda, A.M.S. (2022c), "Nonlinear vibrations of variable thickness curved panels made of multi-scale epoxy/fiberglass/CNT material using Jacobi elliptic functions", *Mech. Based Des. Struct.*, **50**(7), 2333-2349. https://doi.org/10.1080/15397734.2020.1777156.

Mirjavadi, S.S., Khan, I., Forsat, M., Barati, M.R. and Hamouda, A.M.S. (2023), "Analyzing nonlinear vibration of metal foam stiffened toroidal convex/concave shell segments considering porosity distribution", *Mech. Based Des. Struct.*, **51**(1), 310-326. https://doi.org/10.1080/15397734.2020.1841654.

Mirjavadi, S.S., Yahya, Y.Z., Forsat, M., Khan, I., Hamouda, A.M.S. and Barati, M.R. (2020e), "Magneto-electric effects on nonlocal nonlinear dynamic characteristics of imperfect multi-phase magneto-electro-elastic beams", *J. Magn. Magn. Mater.*, **503**, 166649. https://doi.org/10.1016/j.jmmm.2020.166649.

Mousavi, S.M., Shafiei, N. and Dadvand, A. (2017), "Numerical simulation of subsonic turbulent flow over NACA0012 airfoil: evaluation of turbulence models", *Sigma J. Eng. Natural Sci.*, **35**(1), 133-155.

Omidi, S., Oskooee, M.B. and Shafiei, N. (2013), "Finite element analysis of an ultra-fine grained Titanium dental implant covered by different thicknesses of hydroxyapatite layer", *Indian J. Dent.*, **4**(1), 1-4. https://doi.org/10.1016/j.ijd.2012.10.002.

Qi, L., Wang, Z., Sun, Y., Khorami, M., Mahmoudi, T. and Wu, H. (2024), "Modified couple stress and artificial intelligence examination of nonlinear buckling in porous variable thickness cylinder micro sport structures", *Mech. Based Des. Struct.*, 1-19. https://doi.org/10.1080/15376494.2024.2316795.

Shahabinejad, E., Shafiei, N. and Ghadiri, M. (2018), "Influence of temperature change on modal analysis of rotary functionally graded nano-beam in thermal environment", *J. Solid Mech.*, **10**(4), 779-803. https://jsm.arak.iau.ir/article_545719.html.

Shen, B., Xiao, S., Yu, C., Zhang, C., Zhan, J., Liu, Y. and Fu, W. (2024), "Cerebral hemodynamics underlying ankle force sense modulated by high-definition transcranial direct current stimulation", *Cerebral Cortex*. **34**(6), bhae226. https://doi.org/10.1093/cercor/bhae226.

Shi, X., Li, J. and Habibi, M. (2022), "On the statics and dynamics of an electro-thermo-mechanically porous GPLRC nanoshell conveying fluid flow", *Mech. Based Des. Struct.*, **50**(6), 2147-2183. https://doi.org/10.1080/15397734.2020.1772088.

Song, G., Zou, Y., Nie, Y., Habibi, M., Albaijan, I. and Toghroli, E. (2024), "Application of Hashin–Shtrikman bounds homogenization model for frequency analysis of imperfect FG bio-composite plates", *J. Mech. Behav. Biomed. Mater.*, **151**, 106321. https://doi.org/10.1016/j.jmbbm.2023.106321.

Wang, C., Habibi, M. and Mahmoudi, T. (2024a), "Stability analysis of the nonuniform functionally graded cylindrical small-scale beam structures: Application in sport structures", *Steel Compos. Struct.*, **52**(1), 15-29. https://doi.org/10.12989/scs.2024.52.1.015.

Wang, D., Bai, Y., Habibi, M. and Mahmoudi, T. (2024b), "Stability behaviors and governing equations of the volleyball game ball via GDQ and analytical methods", *Adv. Concr. Constr.*, **18**(6), 379-388. https://doi.org/10.12989/acc.2024.18.6.379.

Wang, D., Bai, Y., Habibi, M. and Mahmoudi, T. (2024a), "Stability behaviors and governing equations of the volleyball game ball via GDQ and analytical methods", *Adv. Concr. Constr.*, **18**(6), 379. https://doi.org/10.12989/acc.2024.18.6.379.

Wang, D., Feng, B., Liu, X., Habibi, M. and Mahmoudi, T. (2025a), "Nanoparticle-infused oils for improved lubrication and wear resistance in internal combustion engines: Exploring nanoscience applications in automotive parts", *Adv. Nano Res.*, **18**(1), 1. https://doi.org/10.12989/anr.2025.18.1.001.

Wang, D., Feng, B., Liu, X., Habibi, M. and Mahmoudi, T. (2025b), "Nanoparticle-infused oils for improved lubrication and wear resistance in internal combustion engines: Exploring nanoscience applications in automotive parts", *Adv. Nano Res.*, **18**(1), 1-10. https://doi.org/10.12989/anr.2025.18.1.001.

Wang, D., Wang, Q. and Habibi, M. (2024c), "Electro-magneto-elastic analysis of a sandwich composite beam as diving board in swimming with composed of graphene origami metamaterials", *Mech. Based Des. Struct.*, 1-15. https://doi.org/10.1080/15376494.2024.2422579.

Wang, F., Gao, S., Habibi, M. and Luo, Z. (2024d), "Energy absorption of vibrating sport equipment used for testing athlete performance", *Adv. Nano Res.*, **17**(5), 421-434. https://doi.org/10.12989/anr.2024.17.5.421.

Wang, J., Chen, Y. and Zou, Q. (2023), "Inferring gene regulatory network from single-cell transcriptomes with graph autoencoder model", *PLOS Genetics*, **19**(9), e1010942. https://doi.org/10.1371/journal.pgen.1010942.

Wang, L., Habibi, M. and Huang, G. (2024e), "Smart analysis of sandwich foldable cylinders as gymnastic accessories", *Mech. Based Des. Struct.*, 1-18. https://doi.org/10.1080/15376494.2024.2411414.

Wang, N., Zhang, T., Yang, J., Habibi, M. and Feng, J. (2024f), "Electro-magneto-mechanical critical load analysis of piezo-electric/piezomagnetic sport force plates used for testing athlete performance", *Mech. Based Des. Struct.*, 1-15. https://doi.org/10.1080/15376494.2024.2414944.

Wang, P., Gao, Z., Pan, F., Moradi, Z., Mahmoudi, T. and Khadimallah, M.A. (2022), "A couple of GDQM and iteration techniques for the linear and nonlinear buckling of bi-directional functionally graded nanotubes based on the nonlocal strain gradient theory and high-order beam theory", *Eng. Anal. Bound. Elem.*, **143**, 124-136. https://doi.org/10.1016/j.enganabound.2022.06.007.

Wang, T., Karimi, H.R., Wang, H., Xu, N., Li, L. and Zhao, X. (2025c), "A reinforcement learning methodology to hierarchical sliding-mode surface control of nonlinear systems via a dynamic event-triggered mechanism", *Asian J. Control*, **n/a**(n/a). https://doi.org/10.1002/asjc.3569.

Wang, W., He, C., Xie, L. and Peng, Q. (2019), "The temperature-sensitive anisotropic negative poisson's ratio of carbon honeycomb", *Nanomaterials*, **9**(4). https://doi.org/10.3390/nano9040487.

Wang, W., Zhang, J., Habibi, M. and Albaijan, I. (2024b), "Stretchable-thickness model for dynamic responses of graphene origami reinforced badminton sport plate", *Mech. Based Des. Struct.*, 1-13. https://doi.org/10.1080/15376494.2024.2373976.

Wang, Y., Zhai, Y., Ding, Y. and Zou, Q. (2024g), "SBSM-Pro: support bio-sequence machine for proteins", *Sci. China Inform. Sci.*, **67**(11), 212106. https://doi.org/10.1007/s11432-024-4171-9.

Wang, Y., Zhang, X., Ju, Y., Liu, Q., Zou, Q., Zhang, Y., Ding, Y. and Zhang, Y. (2024h), "Identification of human microRNA-disease association via low-rank approximation-based link propagation and multiple kernel learning", *Front. Comput. Sci.*, **18**(2), 182903. https://doi.org/10.1007/s11704-023-2490-5.

Wu, Q., Zou, S., Liu, W., Liang, M., Chen, Y., Chang, J., Liu, Y. and Yu, X. (2023), "A novel onco-cardiological mouse model of lung cancer-induced cardiac dysfunction and its application in identifying potential roles of tRNA-derived small RNAs", *Biomed. Pharmacotherapy*, **165**, 115117. https://doi.org/10.1016/j.biopha.2023.115117.

Wu, Y., Liang, H., Zhao, N. and Niu, B. (2024), "Low-computation-based adaptive self-triggered bipartite consensus control for nonlinear multiagent systems subject to sensor faults", *IEEE T. Control Netw. Syst.*, **11**(4), 2114-2125. https://doi.org/10.1109/TCNS.2024.3373132.

Xia, L.X., Xiao, Y.Y., Jiang, W.J., Yang, X.Y., Tao, H., Mandukhail, S.R., Qin, J.F., Pan, Q.R., Zhu, Y.G., Zhao, L.X., Huang, L.J., Li, Z. and Yu, X.Y. (2024), "Exosomes derived from induced cardiopulmonary progenitor cells alleviate acute lung injury in mice", *Acta Pharmacologica Sinica*, **45**(8), 1644-1659. https://doi.org/10.1038/s41401-024-01253-4.

Xiao, H., Habibi, M. and Habibi, M. (2024), "Bulk wave propagation analysis of imperfect FG bio-composite beams resting on variable elastic medium", *Mater. Today Commun.*, **39**, 108524. https://doi.org/10.1016/j.mtcomm.2024.108524.

Xue, L., Habibi, M. and Ou, C. (2024), "Stability and instability in responses of a concrete disk with non-classical boundary conditions", *Adv. Concr. Constr.*, **18**(5), 355. https://doi.org/10.12989/acc.2024.18.5.355.

Yan, C., Zhang, T., Zheng, T. and Mahmoudi, T. (2024), "Stability characteristic of bi-directional FG nano cylindrical imperfect composite: Improving the performance of sports bikes using carbon nanotubes", *Steel Compos. Struct.*, **50**(4), 459-474. https://doi.org/10.12989/scs.2024.50.4.459.

Yang, S., Liu, Y., Wu, T., Zhang, X., Xu, S., Pan, Q., Zhu, L., Zheng, P., Qiao, D. and Zhu, W. (2025), "Synthesis and application of a novel multifunctional nanoprodrug for synergistic chemotherapy and phototherapy with hydrogen sulfide gas", *J. Med. Chem.*, **68**(3), 3197-3211. https://doi.org/10.1021/acs.jmedchem.4c02426.

Ye, M., Zhou, Y., Zhao, H. and Wang, X. (2023), "Magnetic microrobots with folate targeting for drug delivery", *Cyborg Bionic Syst.*, **4**, 0019. https://doi.org/10.34133/cbsystems.0019.

Yu, C., Lin, P., Wu, Z., Habibi, M. and Zhang, W. (2024), "Multi-load effect on the deformation analysis of composite nano reinforced origami sandwich panel", *Mech. Based Des. Struct.*, 1-19. https://doi.org/10.1080/15376494.2024.2367015.

Zhang, D., Huang, X., Wang, T., Habibi, M., Albaijan, I. and Toghroli, E. (2024a), "Dynamic stability improvement in spinning FG-piezo cylindrical structure using PSO-ANN and firefly optimization algorithm", *Mater. Sci. Eng. B*, **302**, 117210. https://doi.org/10.1016/j.mseb.2024.117210.

Zhang, H., Habibi, M. and Zou, Y. (2024b), "Static analysis of foldable pressurized and thermally loaded cylindrical shell as an expander in sport equipment reinforced by G-Ori nanofillers", *Mech. Based Des. Struct.*, 1-13. https://doi.org/10.1080/15376494.2024.2412307.

Zhang, L., Chen, Z., Habibi, M., Ghabussi, A. and Alyousef, R. (2021), "Low-velocity impact, resonance, and frequency responses of FG-GPLRC viscoelastic doubly curved panel", *Compos. Struct.*, **269**, 114000. https://doi.org/10.1016/j.compstruct.2021.114000.

Zhang, P., Song, J. and Mahmoudi, T. (2023a), "Simulation and modeling for stability analysis of functionally graded non-uniform pipes with porosity-dependent properties", *Steel Compos. Struct.*, **48**(2), 235-250. https://doi.org/10.12989/scs.2023.48.2.235.

Zhang, Q., Xie, M., Zhou, D., Habibi, M. and Khorami, M. (2024c), "Bending responses of graphene nanoplatelets reinforced sandwich cylindrical micro panel with piezoelectric layers", *Mech. Based Des. Struct.*, 1-16. https://doi.org/10.1080/15376494.2024.2385008.

Zhang, X., Li, J., Cui, Y., Habibi, M., Ali, H.E., Albaijan, I. and Mahmoudi, T. (2023b), "Static analysis of 2D-FG nonlocal porous tube using gradient strain theory and based on the first and higher-order beam theory", *Steel Compos. Struct.*, **49**(3), 293-306. https://doi.org/10.12989/scs.2023.49.3.293.

Zhang, Z., Du, J. and Mahmoudi, T. (2023c), "Green synthesis of silver nanoparticles to the microbiological corrosion deterrence of oil and gas pipelines buried in the soil", *Adv. Nano Res.*, **15**(4), 355-366. https://doi.org/10.12989/anr.2023.15.4.355.

Zhao, C., Kang, J., Li, Y., Wang, Y., Tang, X. and Jiang, Z. (2023), "Carbon-based stimuli-responsive nanomaterials: classification and application", *Cyborg Bionic Syst.*, **4**, 0022. https://doi.org/10.34133/cbsystems.0022.

Zhao, J., Wan, L., Habibi, M. and Brahmia, A. (2024), "An adaptive neuro-fuzzy approach using IoT data in predicting springback in ultra-thin stainless steel sheets with consideration of grain size", *Adv. Nano Res.*, **17**(2), 109. https://doi.org/10.12989/.2024.17.2.109.

Zhao, J., Xu, N., Niu, B., Zhao, X. and Alorfix, A.S. (2025),

"Dynamic event-triggered optimal control for stochastic interconnected nonlinear systems with matched disturbances via adaptive dynamic programming", *J. Franklin Inst.*, **362**(2), 107360. https://doi.org/10.1016/j.jfranklin.2024.107360.

Zhiqiang, S., Aiyun, L., Daichang, Z., Shuangjun, L., Habibi, M., Xiaoling, F. and Albaijan, I. (2024), "Application of a folded nanostructure reinforcement for the pole vault curved shell", *Mech. Based Des. Struct.*, 1-15. https://doi.org/10.1080/15376494.2024.2375368.

Zhou, J., Zhou, L., Chen, Z.Y., Sun, J., Guo, X.W., Wang, H.R., Zhang, X.Y., Liu, Z.R., Liu, J., Zhang, K. and Zhang, X. (2025), "Remineralization and bacterial inhibition of early enamel caries surfaces by carboxymethyl chitosan lysozyme nanogels loaded with antibacterial drugs", *J. Dent.*, **152**, 105489. https://doi.org/10.1016/j.jdent.2024.105489.

Zhu, J., Wang, Y., An, N., Habibi, M. and Wang, H. (2024a), "Application of G-Ori metamaterials as sports equipment baseball bat in an electro-magneto-elastic sandwich composite beam", *Mech. Based Des. Struct.*, 1-20. https://doi.org/10.1080/15376494.2024.2414198.

Zhu, K., Ma, W., Dong, J., Chen, M., Habibi, M. and Albaijan, I. (2024b), "On the dispersion of bulk wave in hygrothermally affected poroelastic gymnastics beams based on refined higher-order shear deformation theory during athlete training", *Mech. Based Des. Struct.*, 1-10. https://doi.org/10.1080/15376494.2024.2428830.

Zhu, L., Ren, H., Habibi, M., Mohammed, K.J. and Khadimallah, M.A. (2022), "Predicting the environmental economic dispatch problem for reducing waste nonrenewable materials via an innovative constraint multi-objective Chimp Optimization Algorithm", *J. Clean. Prod.*, **365**, 132697. https://doi.org/10.1016/j.jclepro.2022.132697.

Zisong, Z. and Habibi, M. (2024), "AI-assisted prediction of St14 steel sheets formability: Neural-fuzzy systems and crystal plasticity assessments", *Structures*, **65**, 106633. https://doi.org/10.1016/j.istruc.2024.106633.